TISSUE ENGINEERING: Part A
Volume 00, Number 00, 2016

DOI: 10.1089/ten.tea.2016.0306

termis
Tissue Engineering
& Regenerative Medicine
International Society

ORIGINAL ARTICLE

Effects of Hydrogel Stiffness and Extracellular Compositions on Modulating Cartilage Regeneration by Mixed Populations of Stem Cells and Chondrocytes *In Vivo*

Tianyi Wang, MS,[1] Janice H. Lai, PhD,[2] and Fan Yang, PhD[1,3]

Cell-based therapies offer great promise for repairing cartilage. Previous strategies often involved using a single cell population such as stem cells or chondrocytes. A mixed cell population may offer an alternative strategy for cartilage regeneration while overcoming donor scarcity. We have recently reported that adipose-derived stem cells (ADSCs) can catalyze neocartilage formation by neonatal chondrocytes (NChons) when mixed co-cultured in 3D hydrogels *in vitro*. However, it remains unknown how the biochemical and mechanical cues of hydrogels modulate cartilage formation by mixed cell populations *in vivo*. The present study seeks to answer this question by co-encapsulating ADSCs and NChons in 3D hydrogels with tunable stiffness (~1–33 kPa) and biochemical cues, and evaluating cartilage formation *in vivo* using a mouse subcutaneous model. Three extracellular matrix molecules were examined, including chondroitin sulfate (CS), hyaluronic acid (HA), and heparan sulfate (HS). Our results showed that the type of biochemical cue played a dominant role in modulating neocartilage deposition. CS and HA enhanced type II collagen deposition, a desirable phenotype for articular cartilage. In contrast, HS promoted fibrocartilage phenotype with the upregulation of type I collagen and failed to retain newly deposited matrix. Hydrogels with stiffnesses of ~7–33 kPa led to a comparable degree of neocartilage formation, and a minimal initial stiffness was required to retain hydrogel integrity over time. Results from this study highlight the important role of matrix cues in directing neocartilage formation, and they offer valuable insights in guiding optimal scaffold design for cartilage regeneration by using mixed cell populations.

Keywords: stem cells, chondrocytes, hydrogel, stiffness, biochemical, cartilage

Introduction

Osteoarthritis is a leading cause of pain and disability among adults.[1] Osteoarthritis arise from focal cartilage defects that may be caused by disease processes, sport-related injuries, or trauma.[1] Unlike most tissues in the human body, cartilage is avascular and is characterized by limited self-healing capacity on injury.[2] Despite extensive efforts over the past few decades, cartilage repair remains a great challenge.[3] Cell-based therapies hold great promise for cartilage repair using chondrocytes or stem cells.[4] However, current cell-based therapies require a large number chondrocytes, which is limited by donor scarcity. Moreover, *in vitro* expansion of chondrocytes results in dedifferentiation and loss of phenotype, leading to the formation of mechanically inferior fibrocartilage.[5,6] Alternatively, stem cells, especially adipose-derived stem cells (ADSCs), offer an attractive cell source for cartilage repair given their availability and potential for proliferation and chondrogenic differentiation.[7,8]

Various strategies have been employed to direct the differentiation of ADSCs both *in vitro* and *in vivo*, including using growth factors or insoluble cell niche cues.[8–11] However, the cartilage regeneration potential of ADSCs alone is still limited.[12] In addition to directly differentiating stem cells into chondrocytes, stem cells may also contribute to cartilage repair indirectly via paracrine signaling to catalyze chondrocytes to produce more neocartilage during co-culture.[13–15] Using a 3D co-culture model in biomimetic hydrogels, we have recently reported that ADSCs can catalyze cartilage formation by neonatal chondrocytes (Nchons), which allows a dramatic reduction of the number of chondrocytes needed for robust articular cartilage formation.[13] These results highlight the

[1]Department of Bioengineering, Stanford University, Stanford, California.
[2]Department of Mechanical Engineering, Stanford School of Medicine, Stanford, California.
[3]Department of Orthopaedic Surgery, Stanford University, Stanford, California.

promise of harnessing the synergistic interactions between stem cells and chondrocytes for cartilage repair. However, how matrix cues, such as biochemical composition and mechanical stiffness, modulate such catalyzed neocartilage formation *in vivo* remains unknown.

Previous studies have suggested that decreasing hydrogel stiffness to lower than 500 Pa generally leads to a more permissive niche for encapsulated cells in 3D and promote more cartilage deposition.[16] Furthermore, extracellular matrix (ECM) compositions such as chondroitin sulfate (CS) and hyaluronic acid (HA) have been shown to enhance cartilage formation by either stem cells or chondrocytes both *in vitro* and *in vivo*.[17–19] However, few studies have directly compared the efficacy of different ECM molecules in modulating cartilage formation in 3D. In addition, heparan sulfate (HS) is a ECM molecule that plays an important role in sequestering growth factors for enhanced cellular activities.[20,21] Given that the synergistic interaction between stem cells and chondrocytes is mediated by paracrine signaling, HS may potentially modulate this interaction by binding to the secreted growth factors. The effects of HS on modulating chondrogenesis have not been well studied, and it remains unknown how different ECM molecules will influence cartilage formation by mixed cell populations.

The present study seeks to answer this question by co-encapsulating ADSCs and NChons in 3D hydrogels with tunable stiffness (0.6 kPa–33 kPa) and biochemical cues, and evaluating cartilage formation *in vivo* using a mouse subcutaneous model. Three ECM molecules were examined, including CS, HA, and HS. We have recently reported development of ECM-containing hydrogels with largely decoupled biochemical and mechanical properties that enabled hydrogel mechanical stiffness to be changed by changing the concentration of poly(ethylene glycol) dimethacrylate (PEGDMA).[12] This system also facilitated switching the type of biochemical cues without significantly altering mechanical stiffness. A total of five groups were studied. ADSCs and NChons were mixed in a 3:1 ratio and encapsulated in the aforementioned hydrogel compositions. Cell-laden hydrogels were implanted subcutaneously into a nude mouse model and harvested at day 21 and 56 to analyze short- and long-term efficacy. Cartilage formation was evaluated by mechanical testing, biochemical assays, and histology.

Materials and Methods

Synthesis of methacrylated ECM molecules

Unless otherwise stated, all chemicals used in the methacrylation of ECM molecules were purchased from Sigma.

CS methacrylate was synthesized by modifying a previously reported method.[22] Briefly, CS sodium salt was reacted with N-hydroxysuccinimide (NHS), and 1-ethyl-3-(3-dimethylaminopropyl)-carbodiimide (EDC) in an MES buffer for 5 min before 2-aminoethyl methacrylate (AEMA) was added. NHS, EDC, and AEMA were reacted at a molar ratio of 1: 2: 1 for 24 h at room temperature, and they were then dialyzed against water for 4 days, lyophilized, and stored at −20°C. HS-methacrylate was synthesized by following the same protocol, replacing CS by HS.

HA methacrylate was synthesized by modifying previously reported methods.[23,24] Briefly, triethylamine and glycidyl methacrylate was added to 20 k MW sodium hyaluronate (Lifecore, Chaska, MN) and reacted for 24 h at room temperature before acetone precipitation. The precipitate was then dissolved and dialyzed against water for 4 days, lyophilized, and stored at −20°C until use.

Details of quantities of reagents used for synthesizing each ECM molecule are shown in Supplementary Table S1 (Supplementary Data are available online at www.liebertpub.com/tea).

Cell isolation and culture

Human ADSCs were isolated from excised human adipose tissue with informed consent by using the method described by Zuk *et al.*[25] hADSCs were expanded for four passages in high-glucose Dulbecco's modified Eagle's medium (DMEM) (Gibco, Invitrogen, Carlsbad, CA) that was supplemented with 10 ng/mL basic fibroblast growth factor (FGFs; PeproTech, Rocky Hill, NJ), 10% (v/v) fetal bovine serum (Gibco, Invitrogen, Carlsbad, CA), 100 U/mL penicillin, and 0.1 mg/mL streptomycin (Gibco, Invitrogen, Carlsbad, CA) and they were used as passage 5 hADSCs in all experiments.

NChons were isolated from the hyaline articular cartilage located at the femoropatellar groove of the stifle joints of a 4-day-old calf (Research 87, Marlborough, MA). Dissected cartilage was further cut into smaller pieces and digested in 1 mg/mL each of collagenase type II and type IV (Worthington Biochemical Lakewood, NJ) supplemented DMEM (Gibco, Invitrogen, Carlsbad, CA) supplemented with 100 U/mL penicillin and 0.1 mg/mL streptomycin (Gibco, Invitrogen, Carlsbad, CA) for 24 h at 37°C. After that, the cell suspension obtained was filtered through a 70 μm nylon mesh, washed with DPBS, and centrifuged. Cells were counted, suspended in freezing media, frozen, and stored in liquid nitrogen as passage 0 NChons.

3D hydrogel formation

Five hydrogel combinations of varying mechanical stiffness and biochemical cues were used in this study (Supplementary Table S2). To vary the stiffness of CS-containing hydrogels, PEGDMA (MW 4.6 kDa) was dissolved in chondrogenic media that was supplemented with 600 ng/mL of TGF-β3 (PeproTech, Rocky Hill, NJ) to achieve final concentrations of 8%, 11%, and 14% (w/v). To vary the biochemical cues, methacrylated ECM molecules (CS, HA, and HS) were incorporated at 2.5% (w/v) in PEGDMA hydrogel [11% (w/v)], which was dissolved in chondrogenic medium supplemented with 600 ng/mL of TGF-β3. 0.05% (w/v) Lithium phenyl-2,4,6-trimethylbenzoylphosphinate was added to hydrogel pre-cursor solutions to act as a photoinitator. Cells were added to the hydrogel precursor solution, and the resulting cell-hydrogel mixture was then pipetted into a 96-well mold and exposed to UV light (365 nm) for 3 min at 4 mW/cm^2 for photocrosslinking. Acellular hydrogels were made accordingly as controls.

Chondrogenic media are composed of high-glucose DMEM (Gibco, Invitrogen, Carlsbad, CA) containing 100 nM dexamethasone (Sigma-Aldrich, St. Louis, MO), 50 mg/mL ascorbate-2-phosphate (Sigma-Aldrich, St. Louis, MO), 40 mg/mL proline (Sigma-Aldrich, St. Louis, MO), 100 mg/mL sodium pyruvate (Gibco, Invitrogen, Carlsbad, CA), 100 U/mL penicillin, 0.1 mg/mL streptomycin (Invitrogen,

Carlsbad, CA), 5 μg/mL ITS Premix (BD Biosciences, San Jose, CA), and 600 ng/mL of TGF-β (PeproTech, Rocky Hill, NJ).

Implantation into subcutaneous nude mice model

Animal studies were performed in accordance with the guidelines for the care and use of laboratory animals; all protocols were approved by the Stanford institutional animal care and use committee.

Before encapsulation, passage 4 hADSCs were trypsinized and counted. NChons were thawed from their storage in liquid nitrogen and counted without further expansion. The mixed cell population consisting of hADSCs and NChons in a 3: 1 ratio was homogenously mixed with the hydrogel pre-cursor solution at 15 million cells/mL. After photocrosslinking, each 50 μL cell-hydrogel construct was directly implanted into nude mice subcutaneously (NCRNU, 9 weeks, Taconic). Mice were sacrificed to obtain cell-hydrogel constructs after 21 and 56 days *in vivo*. A total of eight samples were evaluated for each group. Outcomes were analyzed by using mechanical testing ($n > 6$), biochemical assays for DNA, sulfated glycosaminoglycan (sGAG), and hydroxyproline ($n = 5$), as well as immunostaining ($n = 3$).

Mechanical testing

Unconfined compression tests were conducted by using an Instron 5944 materials testing system (Instron Corporation, Norwood, MA) fitted with a 10 N load cell (Interface, Inc., Scottsdale, AZ). A custom-made aluminum compression plate lined with PTFE was used to minimize friction. Specimen diameter and thickness were measured. A 10 mN preload was applied before each test, and the upper plate was then lowered at a rate of 1% strain/sec. The compressive modulus was determined from 10% to 20% of linear curve fit from the stress versus strain curve. Mechanical stiffness of day 1, 21, and 56 harvested cell-laden hydrogels was measured. All tests were conducted in phosphate-buffered saline solution at room temperature.

Biochemical assays

After 21 and 56 days postimplantation, cell-laden hydrogels ($n = 5$) were harvested and their wet weights were obtained. They were then lyophilized to obtain their dry weights. The lyophilized hydrogels were then each digested in 500 μL of papainase solution (Worthington Biochemical, Lakewood, NJ) at 60°C for 16 h. The supernatant was then used for the following biochemical assays.

DNA content was measured by using the Quant-iT PicoGreen dsDNA Assay Kit (Molecular Probes, Eugene, OR) following the manufacturer's protocol, using Lambda phage DNA as standard. sGAG content was quantified spectrophotometrically by using the 1,9-imethylmethylene blue (DMMB) dye-binding assay (pH 3.0) using shark CS (Sigma, St. Louis, MO) as the standard. Total collagen content was determined by using the Ehrlich's reaction assay for hydroxyproline as previously described.[26] Briefly, acid hydrolysis was performed whereby concentrated hydrochloric acid was added to 50 μL of supernatant and reacted at 110°C for 16 h. Samples were then dried under a sodium hydroxide ice-trap under vacuum conditions. The dried samples were then reconstituted in water and reacted with p-dimethylaminobenzaldehyde and chloramine T (Sigma, St. Louis, MO). Absorbance of samples was read at 540 nm after a 20 min incubation at 60°C, and it was compared with a hydroxyproline standard. Collagen content was estimated by assuming 1: 7.46 hydroxyproline: collagen mass ratio[26]

Histology

After harvesting the cell-hydrogel constructs ($n = 3$), samples were fixed in 4% (w/v) paraformaldehyde (Sigma, St. Louis, MO) for 1 h at room temperature and then immersed in a 30% (w/v) sucrose solution overnight at 4°C. Samples were then snap frozen in Optimal Cutting Temperature solution and then stored at −80°C. Cryosectioning was performed at −20°C.

To visualize the amount and distribution of types I, II, and X collagen, immunostaining was performed. Enzymatic antigen retrieval was performed by incubating sections in 0.1% trypsin (Gibco, Invitrogen, Carlsbad, CA) at 37°C for 15 min. Sections were subsequently blocked with blocking buffer consisting of 2% (v/v) goat serum (Gibco, Invitrogen, Carlsbad, CA) and 3% (w/v) bovine serum albumin (Fisher Scientific, Pittsburgh, PA) for 1 h at room temperature. For primary staining, rabbit polyclonal antibody to collagens type I, II, or X (Abcam, Cambridge, MA) was added to the sections and incubated overnight at 4°C. For secondary staining, Alexa Fluor 488 goat anti-rabbit (Invitrogen, Carlsbad, CA) was added to the sections and then incubated for 1 h at room temperature. Cell nuclei were counterstained with Hoechst dye 33342 (Cell Signaling Technologies, Danvers, MA) for 1 h at room temperature. Sections were then mounted with vectashield, (Vector Laboratories, Burlingame, CA) and imaged by using a Zeiss fluorescence microscope.

To visualize sGAG amounts and distribution, Safranin-O was counterstained with fast green FCF. Slides were then dehydrated and mounted with permount (Sigma-Aldrich, St. Louis, MO).

Statistical analysis

All experiments are performed with at least three replicates ($n \geq 3$). GraphPad Prism (GraphPad Software, San Diego, CA) was used to perform statistical analysis. Statistical significance was determined by using one- or two-way analysis of variance, and pairwise comparisons with Tukey's *post-hoc* test were used to determine statistical significance ($p < 0.05$).

Results

Mechanical stiffness of hydrogels after in vivo *implantation*

Unconfined compression test was performed on harvested cell-hydrogel constructs after 1 day of *in vitro* culture as control, and after 21 and 56 days of *in vivo* implantation. For CS-containing hydrogels, varying the concentration of PEG from 8% to 14% (w/v) resulted in hydrogels with three distinctive stiffness ranges, including 0.67, 6.90, and 32.70 kPa, respectively. For HA- and HS-containing hydrogels, only the immediate PEG concentration was used, resulting in hydrogels with stiffness in the comparable range as CS hydrogels with intermediate stiffness (Table 1).

Throughout the entire *in vivo* implantation, there were no significant changes in hydrogel mechanical stiffness in both

Table 1. Mean Young's Modulus (kPa) ± Standard Deviation of Hydrogels with Varying Extracellular Matrix Compositions and Varying Mechanical Stiffness on Day 1 (A), and After Day 21 (B) and Day 56 (C) of *In Vivo* Subcutaneous Implantation in Nude Mice

	Day 1			*Day 21*			*Day 56*		
PEGDMA	*CS*	*HA*	*HS*	*CS*	*HA*	*HS*	*CS*	*HA*	*HS*
8%	0.67 ± 0.06	—	—	NA	—	—	NA	—	—
11%	6.90 ± 0.82	12.23 ± 1.29	4.60 ± 1.22	6.20 ± 1.02	11.74 ± 2.14	7.18 ± 1.60	5.66 ± 5.06	12.83 ± 5.06	6.61 ± 5.23
14%	32.70 ± 1.02	—	—	41.87 ± 7.31	—	—	34.34 ± 7.66	—	—

CS, chondroitin sulfate; HA, hyaluronic acid; HS, heparan sulfate; NA, represents not available due to hydrogel degradation; PEGDMA, poly(ethylene glycol) dimethacrylate.

short-term (21 days) and long-term (56 days) implantation, for four hydrogel compositions (Table 1). Mechanical testing data were not available for hydrogels containing 8% (w/v) PEG (~1 kPa) at both 21 and 56 day time points, as these hydrogels disintegrated *in vivo* before day 21.

Modulation of ADSC/NChon interaction in hydrogels

Picogreen DNA assay was performed to quantify the amount of DNA in each hydrogel after 1 day of *in vitro* culture, and after 21 and 56 days of *in vivo* implantation. Our results showed that there was a similar number of cells within each hydrogel at the start of the implantation (Fig. 1A). Cell proliferation occurred in all groups during the first 21 days of *in vivo* implantation. However, only cells in the stiff CS-containing hydrogel group (14% [w/v] PEG, ~33 kPa) continued proliferating between days 21 and 56 of *in vivo* implantation.

The effects of biochemical and mechanical cues on sGAG and collagen production by encapsulated cells *in vivo* are particularly relevant to understanding the influence of niche cues on chondrogenesis. To this end, we analyzed production of sGAG and collagen over short-term (21 days) and long-term (56 days) *in vivo* implantation.

Our data showed that throughout 21 days of *in vivo* implantation, there was a significant increase in sGAG in all groups (Fig. 1B). Among the biochemical cues used in our study, CS-containing hydrogels with a high mechanical stiffness (14% [w/v] PEG, ~33 kPa) resulted in the highest production of sGAG by encapsulated cells after 21 days of implantation. As mechanical stiffness was increased in CS-containing hydrogels from ~7 kPa to ~33 kPa, sGAG production increased by 1.8-fold (Fig. 1B). From day 21 to 56 of implantation, only cells encapsulated in CS- or HA-containing hydrogels, but not those in HS-containing hydrogels, saw significant increases in sGAG amounts. Furthermore, HS-containing hydrogels were the least able to support long-term sGAG accumulation, as sGAG accumulation after 56 days was only ~66% of the other hydrogel compositions (Fig. 1B). Cells encapsulated in all other hydrogel compositions produced similar amounts of sGAG after 56 days of implantation. Our data showed that both biochemical niche cues and mechanical stiffness can modulate neocartilage formation by a mixed population of ADSCs and NChons in 3D hydrogels, with biochemical cues playing a more dominant role.

Similar to sGAG, collagen accumulation also increased significantly from day 1 to 21 (Fig. 1C). Our results showed that neither mechanical nor biochemical cues significantly modulated collagen production by cells in the first 21 days. After 56 days of implantation, both CS- and HA-containing hydrogels supported 2.5–2.7-fold of increase in collagen production as compared with day 21; total secreted collagen in HS-containing hydrogels did not increase significantly from 21 days to 56 days of implantation. This showed that biochemical niche cues were able to modulate long-term collagen deposition by cells.

Histological data

Immunostaining was performed to investigate type and distribution of deposited collagen. All hydrogels were cryosectioned and immunostained for types I, II, and X collagen (Figs. 2 and 3).

Immunostaining and light microscopy data showed that an increase in mechanical stiffness from ~1 kPa to ~33 kPa conferred by increasing PEG concentration from 8% (w/v) to

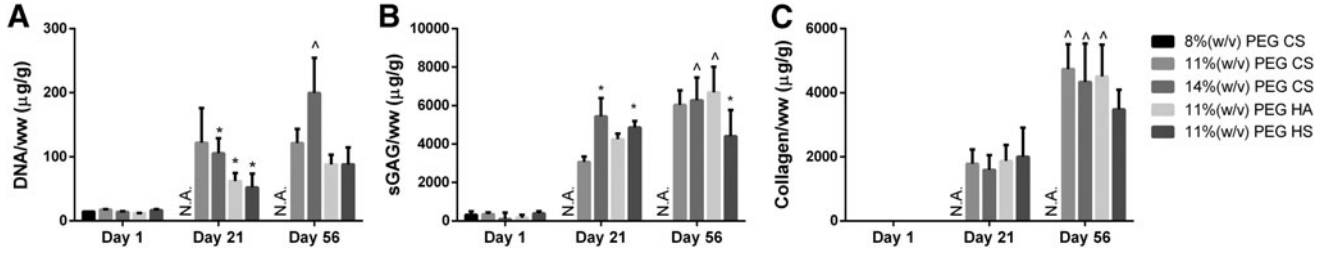

FIG. 1. Biochemical assays to quantify DNA **(A)** sGAG **(B)** and collagen **(C)** accumulation within hydrogels of varying ECM compositions after 21 and 56 days of *in vivo* implantation in nude mice. *Statistical significance as compared with 11% (w/v) PEG CS at the same time point, ^statistical significance between day 21 and 56 for the same hydrogel composition, */^$p < 0.05$. CS, chondroitin sulfate; ECM, extracellular matrix; PEG, poly(ethylene glycol); sGAG, sulfated glycosaminoglycan.

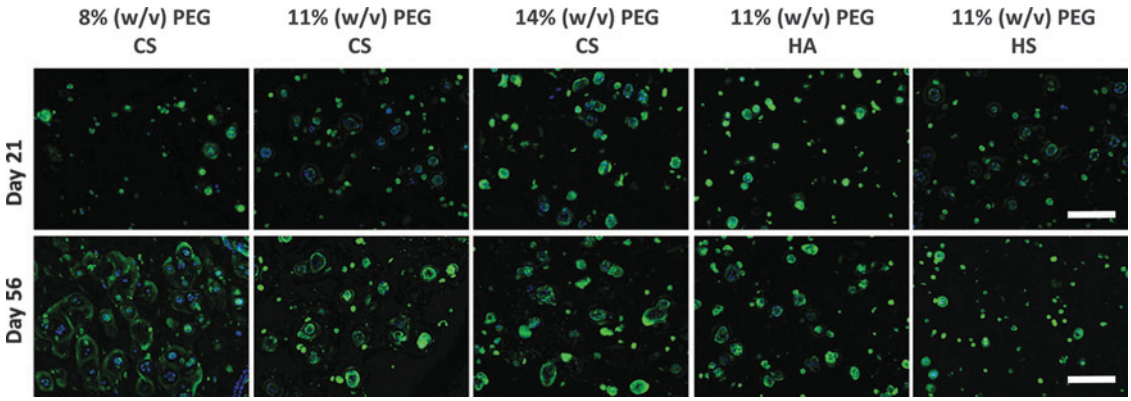

FIG. 2. Immunostaining of articular cartilage marker, type II collagen, to visualize the distribution of newly deposited hyaline cartilage by mixed ADSCs/NChons within hydrogels of varying stiffness and ECM compositions after 21 and 56 days of *in vivo* implantation. Type of ECM molecule had a more dominant effect, and CS/HA generally led to a higher amount of type II collagen than HS. ADSC, adipose-derived stem cells; NChons, neonatal chondrocytes; *Green,* type II collagen; *Blue,* DAPI. Scale bar: 200 μm. HA, hyaluronic acid; HS, heparan sulfate. Color images available online at www.liebertpub.com/tea

14% (w/v) in CS-containing hydrogels resulted in a higher type II collagen staining intensity and larger nodule sizes after 21 days (Fig. 2 and Supplementary Fig. S1). However, after 56 days *in vivo*, nodule sizes were the largest in soft hydrogels (~1 kPa), which contain 8% (w/v) PEG, as compared with hydrogels containing 11% (w/v) and 14% (w/v) PEG (Fig. 2), although with lower staining intensity.

Nodule sizes were different in hydrogels of different biochemical compositions. Specifically, all CS-containing hydrogels had larger type II collagen nodules as compared with those of HA- or HS-containing hydrogels at days 21 and 56 (Fig. 2 and Supplementary Fig. S1). Nodules in CS-containing hydrogels were larger and stained more intensely on day 56 as compared with day 21, whereas nodules in HA-

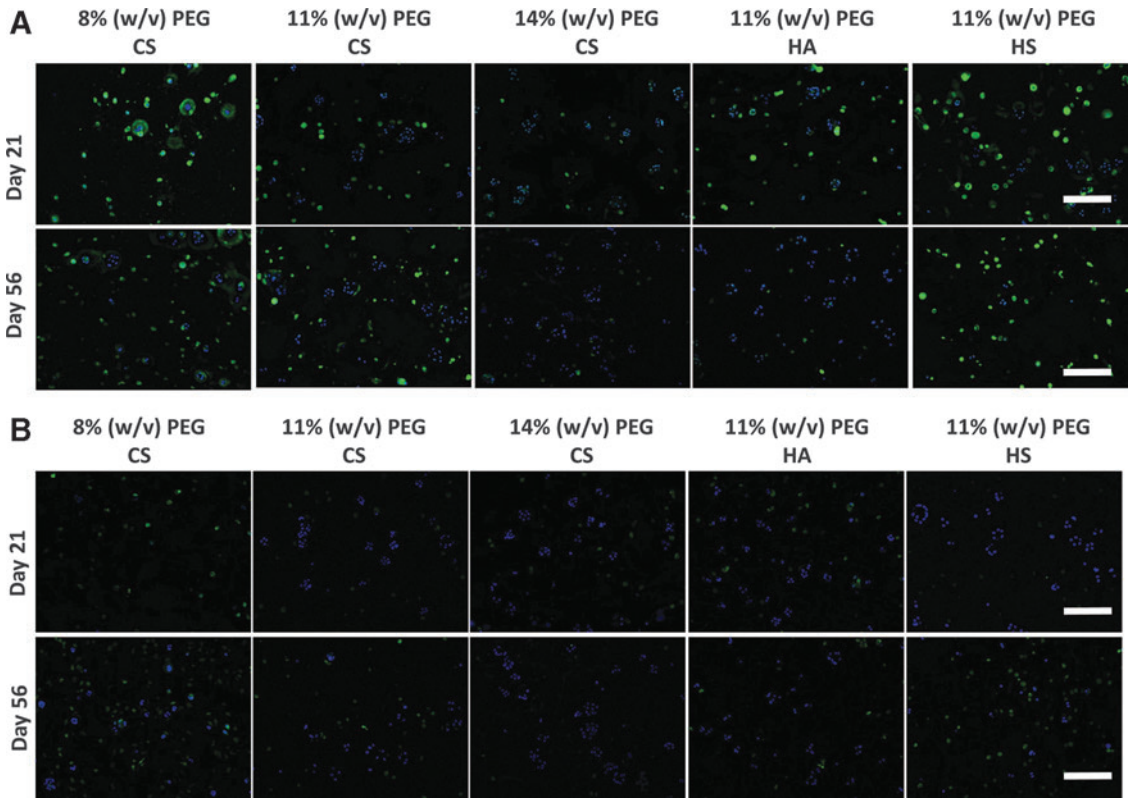

FIG. 3. Immunostaining of fibrocartilage marker, type I collagen **(A)** and hypertrophy marker type X collagen **(B)** by mixed ADSCs/NChons in hydrogels of varying stiffness and ECM compositions after 21 and 56 days of *in vivo* implantation. Soft and intermediate hydrogel stiffness led to some fibrocartilage, which was absent in stiff hydrogels. Minimal hypertrophy phenotype was observed in all groups. *Green,* Collagen, *Blue,* DAPI. Scale bar: 200 μm. Color images available online at www.liebertpub.com/tea

and HS-containing hydrogels remained similar in size from day 21 to 56 of *in vivo* implantation. In particular, nodules were the smallest in HS-containing hydrogel. After 56 days of implantation, nodules in this hydrogel did not increase in size (Supplementary Fig. S1), although the intensity of staining increased slightly (Fig. 2).

Type I collagen production was affected by the hydrogel's mechanical stiffness and biochemical composition. Immunostaining revealed that in CS-containing hydrogels, low mechanical stiffness (~1 kPa) led to significantly higher type I collagen staining (Fig. 3A). As mechanical stiffness increased to ~33 kPa, type I collagen staining decreased to a minimal. This trend was observed at both days 21 and 56 of implantation. Furthermore, immunostaining also showed that HS-containing hydrogels led to higher type I collagen production on both days 21 and 56 as compared with CS- and HA-containing hydrogels. Cells encapsulated in HA-containing hydrogels secreted small amounts of type I collagen after 21 days, which disappeared after 56 days (Fig. 3A).

Type X collagen staining across all hydrogel compositions was minimal as compared with types I and II collagen (Fig. 3B).

Safranin-O staining showed that among CS-containing hydrogels, cells in stiff hydrogels (~33 kPa) deposited the most sGAG nodules 21 days postimplantation (Fig. 4). At 56 days postimplantation, although the number of sGAG nodules in soft hydrogels (~1 kPa) increased significantly from day 21, these nodules had diffuse edges. In contrast, in stiff CS-containing hydrogels (~33 kPa), all sGAG nodules had well-defined edges. Safranin-O staining further showed that the size and number of sGAG nodules increased in both CS- and HA-containing hydrogels from day 21 to 56 but sGAG nodules decreased in both size and number in HS-containing hydrogels (Fig. 4). In addition, sGAG nodules in HS-containing hydrogels had diffuse edges after 21 days of implantation (Fig. 4).

Discussion

Hydrogels are attractive matrices to enhance cell-based therapies for cartilage repair due to their injectability and ease of filling cartilage defects of any shape. We have recently reported that ADSCs can catalyze cartilage formation by Nchons when they are mixed co-cultured in 3D biomimetic hydrogels.[13] The present study seeks to further evaluate the effects of hydrogel compositions and stiffness on modulating such synergistic interactions and neocartilage formation. Three ECM molecules were chosen (CS, HA, and HS) and chemically incorporated into 3D hydrogels at a physiologically relevant concentration (2.5% [w/v]). In addition, we varied the stiffness of CS-containing hydrogels by changing the concentration of bioinert polymer PEG. Previous studies have shown that soft hydrogels generally provide a more permissive environment in enabling encapsulated cells to produce neocartilage in 3D *in vitro* due to the lower number of crosslinks resulting in a less restrictive environment for the cells.[27–29] As such, we have chosen hydrogels with tunable stiffness ranging from ~1 kPa to ~33 kPa. Our results showed that the choice of biochemical cues in hydrogels plays an important role in determining the neocartilage phenotype (articular cartilage vs. fibrocartilage). Increasing hydrogel stiffness from ~7 kPa to ~33 kPa in CS-containing hydrogels accelerated sGAG deposition, an

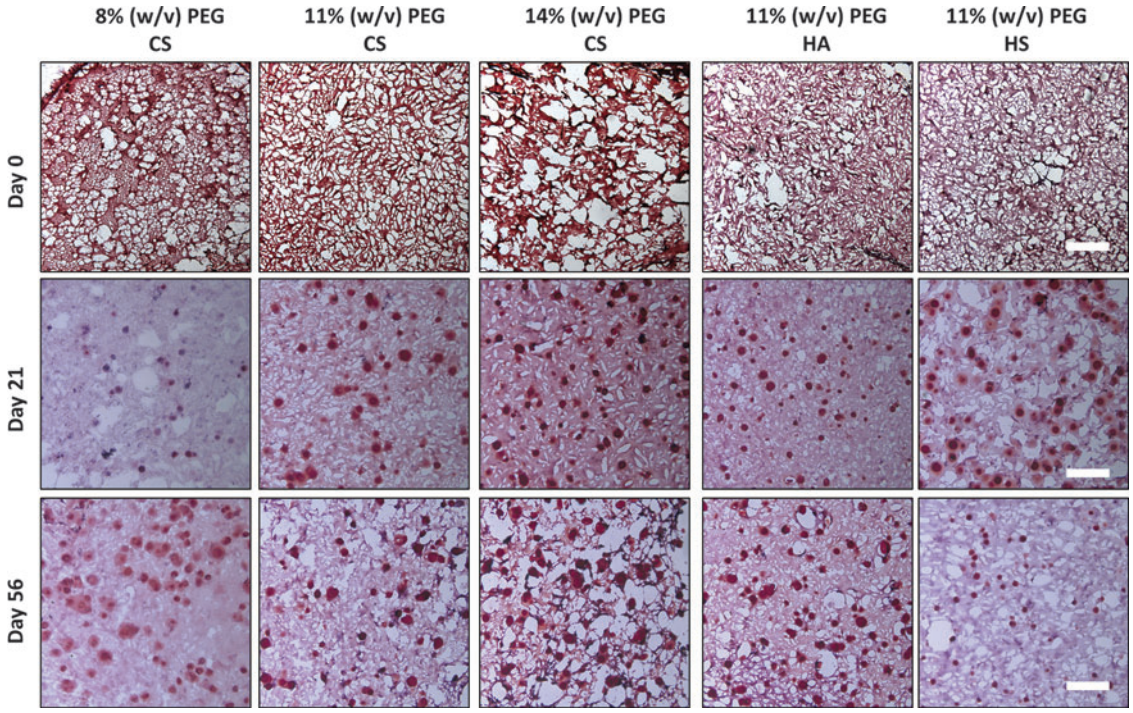

FIG. 4. Safranin-O staining to visualize the amount and distribution of sGAG deposited by mixed ADSCs/NChons within hydrogels of varying stiffness and ECM composition after 21 and 56 days of *in vivo* implantation. Increasing hydrogel stiffness enhanced sGAG deposition. CS led to the greatest sGAG deposition, whereas HS failed to retain sGAG over time. Scale bar: 200 μm. Color images available online at www.liebertpub.com/tea

important component of cartilage ECM. Importantly, soft hydrogel with an initial stiffness of ~1 kPa failed to maintain its structural integrity after implantation. Taken together, these results highlighted the importance of optimizing matrix stiffness for supporting catalyzed cartilage formation *in vivo* by mixed cell populations.

Cartilage functions as a load-bearing tissue in the body with unique shock-absorbing capacities. As such, when choosing matrices to enhance cell-based cartilage regeneration *in vivo*, it is important to evaluate their structural stability after implantation while still supporting cell-based cartilage deposition. In our study, although hydrogels with the lowest stiffness (~1 kPa) led to more extensive and homogeneous neocartilage in 3D hydrogels (Figs. 2 and 4), they were unable to maintain structural integrity and broke into pieces after 21 days of *in vivo* implantation. Thus, this hydrogel composition was unsuitable for supporting cartilage repair *in vivo*. In contrast, hydrogels containing an initial mechanical stiffness of more than ~7 kPa were able to maintain their integrity throughout the 56 days of implantation.

Hydrogel stiffness has been shown to play an important role in modulating cell-based cartilage formation in 3D. Generally, soft hydrogels have been shown to support greater neocartilage deposition by encapsulated cells *in vitro* due to their permissiveness.[16,27,30] Interestingly, our results showed that increasing stiffness of CS-containing hydrogels to ~33 kPa resulted in accelerated sGAG deposition by chondrocytes and ADSCs at day 21 postimplantation (Fig. 1B). However, by day 56, sGAG production in CS-containing hydrogels with a moderate stiffness (~7 kPa) had caught up with that of stiff hydrogels (~33 kPa), as shown by Safranin-O staining for sGAG (Fig. 4).

For articular cartilage regeneration, one challenge is that cells often produce undesirable fibrocartilage rather than the desirable hyaline cartilage phenotype. Immunostaining of fibrocartilage marker, type I collagen, showed that both soft and intermediate stiffness (~1–7 kPa) led to fibrocartilage deposition, whereas minimal fibrocartilage was observed in stiff hydrogels (~33 kPa) (Fig. 3A). Collagen X was absent in all hydrogel compositions and suggested that cells were not hypertrophic (Fig. 3B). Neocartilage deposition was largely pericellular in all hydrogel groups. Consistent with our observations, Nicodemus *et al.* observed pericellular neocartilage deposition when bovine chondrocytes were encapsulated within PEG hydrogels of high crosslinking densities.[28] Taken together, although soft hydrogels allowed greater neocartilage deposition *in vivo*, their lack of mechanical integrity meant that they were unsuitable for *in vivo* implantation. Hydrogels that are ~33 kPa best supported hyaline cartilage deposition by the co-cultured ADSCs/NChons. Results from our study suggested that it would be advantageous to encapsulate cells in stiffer rather than softer hydrogels to ensure an intact hydrogel post-implantation. In addition, although hydrogels with lower crosslinking density and lower mechanical stiffness are more permissive and will enable cells to deposit more neocartilage *in vitro*, structural integrity of the hydrogel is an important parameter to consider for *in vivo* implantation.

CS and HA have been widely used as matrices for guiding cell-based cartilage repair, whereas little is known about the effect of HS on modulating cartilage formation.[18,31–35] To determine the effects of ECM compositions (CS, HA, and HS) on modulating cartilage formation by mixed ADSCs/NChons, we used the same amount of PEG to provide comparable stiffness of hydrogels. All ECM compositions led to a comparable amount of collagen and sGAG deposition at day 21, whereas HS-containing hydrogels failed to retain the matrix over 56 days after implantation (Fig. 1B, C). This result is also supported by Safranin-O staining for sGAG, in which HS-containing hydrogels showed significant loss of sGAG by day 56 compared with day 21 (Fig. 4). In contrast, CS- and HA-containing hydrogels showed increased sGAG deposition over time. Furthermore, HS promoted deposition of type I collagen, which is an undesirable fibrocartilage phenotype (Fig. 3A). HS can bind to a large range of growth factors, including FGFs.[20,36–38] One possible explanation for the observation that HS promoted type I collagen deposition is enhanced and prolonged HS-FGF interactions. Taken together, our results suggest that CS- and HA-containing hydrogels are more suitable for articular cartilage regeneration using mixed ADSC/NChon populations.

Despite the amount of newly deposited cartilage matrix in leading hydrogel compositions (CS and HA), no apparent increase in the stiffness of cell-laden hydrogels was observed after 56 days of implantation *in vivo* (Table 1). The final stiffness of engineered cartilage is a combined result of loss of the original hydrogel stiffness due to degradation, as well as an increase in stiffness as contributed by newly deposited cartilage. Mechanical stiffness will increase appreciably once neocartilage nodules become interconnected after long-term culture to compensate for the loss of original hydrogels. To address this limitation, future work may explore using degradable PEG to provide initial mechanical integrity, while allowing timely degradation to accelerate neocartilage deposition in a more extensive and interconnected manner.[39,40] Finally, we have chosen a mouse subcutaneous model in this study to allow screening of large number of samples for mechanical testing, histology, and biochemical assays. Future studies could further validate leading hydrogel compositions identified from this study in osteochondral defects using larger animal models.

Conclusion

In summary, here we evaluate the effects of varying hydrogel stiffness and ECM compositions on modulating neocartilage deposition by mixed ADSC/NChon *in vivo*. Our results demonstrate that the type of ECM plays a more dominant role in the resulting cartilage phenotype. Both CS- and HA-containing hydrogels support desirable hyaline cartilage phenotype deposition, whereas HS-containing hydrogels promote undesirable fibrocartilage phenotype and failed to retain newly deposited matrix over time. Hydrogels with stiffnesses of 7–33 kPa led to a comparable degree of neocartilage formation, and a minimal initial stiffness was required to retain hydrogel integrity over time. Results from this study highlight the important role of matrix cues in directing neocartilage formation, and they offer valuable insights in guiding optimal scaffold design for cartilage regeneration using mixed cell populations.

Acknowledgments

This work was supported by the following grants: NIH R01DE024772 (F.Y.), NSF CAREER award (CBET-1351289) (F.Y.), and California Institute for Regenerative

Medicine Tools and Technologies Award (RT3-07804) (F.Y.). The authors also acknowledge funding from the Stanford Chem-H Institute (F.Y.), the Stanford Bio-X Interdisciplinary Initiative Program (F.Y.), the Stanford Child Health Research Institute Faculty Scholar Award (F.Y.), and the Alliance for Cancer Gene Therapy Young Investigator award grant (F.Y.). T.W. would like to acknowledge A*STAR (Singapore) for predoctoral fellowship support. The authors would like to thank Anthony Behn for technical assistance in mechanical testing.

Disclosure Statement

No competing financial interests exist.

References

1. Allen, K.D., and Golightly, Y.M. State of the evidence. Current opinion in rheumatology **27,** 276, 2015.
2. Griffin, T.M., and Guilak, F. The role of mechanical loading in the onset and progression of osteoarthritis. Exerc Sport Sci Rev **33,** 195, 2005.
3. Huey, D.J., Hu, J.C., and Athanasiou, K.A. Unlike bone, cartilage regeneration remains elusive. Science **338,** 917, 2012.
4. Mobasheri, A., Kalamegam, G., Musumeci, G., and Batt, M.E. Chondrocyte and mesenchymal stem cell-based therapies for cartilage repair in osteoarthritis and related orthopaedic conditions. Maturitas **78,** 188, 2014.
5. Brittberg, M., Peterson, L., Sjogren-Jansson, E., Tallheden, T., and Lindahl, A. Articular cartilage engineering with autologous chondrocyte transplantation. A review of recent developments. J Bone Joint Surg Am **85-A Suppl 3,** 109, 2003.
6. Redman, S.N., Oldfield, S.F., and Archer, C.W. Current strategies for articular cartilage repair. Eur Cells Mater **9,** 23, 2005; discussion 23.
7. Zuk, P.A., Zhu, M., Mizuno, H., Huang, J., Futrell, J.W., Katz, A.J., *et al.* Multilineage cells from human adipose tissue: implications for cell-based therapies. Tissue Eng **7,** 211, 2001.
8. Estes, B.T., Diekman, B.O., Gimble, J.M., and Guilak, F. Isolation of adipose-derived stem cells and their induction to a chondrogenic phenotype. Nat Protoc **5,** 1294, 2010.
9. Awad, H.A., Wickham, M.Q., Leddy, H.A., Gimble, J.M., and Guilak, F. Chondrogenic differentiation of adipose-derived adult stem cells in agarose, alginate, and gelatin scaffolds. Biomaterials **25,** 3211, 2004.
10. Peran, M., Ruiz, S., Kwiatkowski, W., Marchal, J.A., Yang, S.L., Aranega, A., *et al.* Activin/BMP2 chimeric ligands direct adipose-derived stem cells to chondrogenic differentiation. Stem Cell Res **10,** 464, 2013.
11. Erickson, G.R., Gimble, J.M., Franklin, D.M., Rice, H.E., Awad, H., and Guilak, F. Chondrogenic potential of adipose tissue-derived stromal cells in vitro and in vivo. Biochem Biophys Res Commun **290,** 763, 2002.
12. Wang, T., Lai, J.H., Han, L.H., Tong, X., and Yang, F. Chondrogenic differentiation of adipose-derived stromal cells in combinatorial hydrogels containing cartilage matrix proteins with decoupled mechanical stiffness. Tissue Eng Part A **20,** 2131, 2014.
13. Lai, J.H., Kajiyama, G., Smith, R.L., Maloney, W., and Yang, F. Stem cells catalyze cartilage formation by neonatal articular chondrocytes in 3D biomimetic hydrogels. Sci Rep **3,** 3553, 2013.
14. Meretoja, V.V., Dahlin, R.L., Kasper, F.K., and Mikos, A.G. Enhanced chondrogenesis in co-cultures with articular chondrocytes and mesenchymal stem cells. Biomaterials **33,** 6362, 2012.
15. Hildner, F., Concaro, S., Peterbauer, A., Wolbank, S., Danzer, M., Lindahl, A., *et al.* Human adipose-derived stem cells contribute to chondrogenesis in coculture with human articular chondrocytes. Tissue Eng Part A **15,** 3961, 2009.
16. Murphy, C.M., Matsiko, A., Haugh, M.G., Gleeson, J.P., and O'Brien, F.J. Mesenchymal stem cell fate is regulated by the composition and mechanical properties of collagen-glycosaminoglycan scaffolds. J Mech Behav Biomed Mater **11,** 53, 2012.
17. Varghese, S., Hwang, N.S., Canver, A.C., Theprungsirikul, P., Lin, D.W., and Elisseeff, J. Chondroitin sulfate based niches for chondrogenic differentiation of mesenchymal stem cells. Matrix Biol **27,** 12, 2008.
18. Wang, D.A., Varghese, S., Sharma, B., Strehin, I., Fermanian, S., Gorham, J., *et al.* Multifunctional chondroitin sulphate for cartilage tissue-biomaterial integration. Nat Mater **6,** 385, 2007.
19. Burdick, J.A., and Prestwich, G.D. Hyaluronic acid hydrogels for biomedical applications. Adv Mater **23,** H41, 2011.
20. Kirn-Safran, C.B., Gomes, R.R., Brown, A.J., and Carson, D.D. Heparan sulfate proteoglycans: coordinators of multiple signaling pathways during chondrogenesis. Birth Defects Res C Embryo Today **72,** 69, 2004.
21. Matsuo, I., and Kimura-Yoshida, C. Extracellular distribution of diffusible growth factors controlled by heparan sulfate proteoglycans during mammalian embryogenesis. Philos Trans R Soc Lond B Biol Sci **369,** pii: 20130545, 2014.
22. Jeon, O., Bouhadir, K.H., Mansour, J.M., and Alsberg, E. Photocrosslinked alginate hydrogels with tunable biodegradation rates and mechanical properties. Biomaterials **30,** 2724, 2009.
23. Baier Leach, J., Bivens, K.A., Patrick, C.W., Jr., and Schmidt, C.E. Photocrosslinked hyaluronic acid hydrogels: natural, biodegradable tissue engineering scaffolds. Biotechnol Bioeng **82,** 578, 2003.
24. Suri, S., and Schmidt, C.E. Cell-laden hydrogel constructs of hyaluronic acid, collagen, and laminin for neural tissue engineering. Tissue Eng Part A **16,** 1703, 2010.
25. Zuk, P.A., Zhu, M., Ashjian, P., De Ugarte, D.A., Huang, J.I., Mizuno, H., *et al.* Human adipose tissue is a source of multipotent stem cells. Mol Biol Cell **13,** 4279, 2002.
26. Neuman, R.E., and Logan, M.A. The determination of hydroxyproline. J Biol Chem **184,** 299, 1950.
27. Liu, S.Q., Tian, Q., Hedrick, J.L., Po Hui, J.H., Ee, P.L., and Yang, Y.Y. Biomimetic hydrogels for chondrogenic differentiation of human mesenchymal stem cells to neocartilage. Biomaterials **31,** 7298, 2010.
28. Nicodemus, G.D., Skaalure, S.C., and Bryant, S.J. Gel structure has an impact on pericellular and extracellular matrix deposition, which subsequently alters metabolic activities in chondrocyte-laden PEG hydrogels. Acta Biomater **7,** 492, 2011.
29. Bryant, S.J., Bender, R.J., Durand, K.L., and Anseth, K.S. Encapsulating chondrocytes in degrading PEG hydrogels with high modulus: engineering gel structural changes to facilitate cartilaginous tissue production. Biotechnol Bioeng **86,** 747, 2004.
30. Bian, L., Hou, C., Tous, E., Rai, R., Mauck, R.L., and Burdick, J.A. The influence of hyaluronic acid hydrogel crosslinking density and macromolecular diffusivity on human MSC chondrogenesis and hypertrophy. Biomaterials **34,** 413, 2013.

31. Chen, W.C., Wei, Y.H., Chu, I.M., and Yao, C.L. Effect of chondroitin sulphate C on the in vitro and in vivo chondrogenesis of mesenchymal stem cells in crosslinked type II collagen scaffolds. J Tissue Eng Regen Med **7,** 665, 2013.
32. Coburn, J.M., Gibson, M., Monagle, S., Patterson, Z., and Elisseeff, J.H. Bioinspired nanofibers support chondrogenesis for articular cartilage repair. Proc Natl Acad Sci U S A **109,** 10012, 2012.
33. Bian, L., Guvendiren, M., Mauck, R.L., and Burdick, J.A. Hydrogels that mimic developmentally relevant matrix and N-cadherin interactions enhance MSC chondrogenesis. Proc Natl Acad Sci U S A **110,** 10117, 2013.
34. Xu, X., Jha, A.K., Harrington, D.A., Farach-Carson, M.C., and Jia, X. Hyaluronic acid-based hydrogels: from a natural polysaccharide to complex networks. Soft Matter **8,** 3280, 2012.
35. Kim, I.L., Mauck, R.L., and Burdick, J.A. Hydrogel design for cartilage tissue engineering: a case study with hyaluronic acid. Biomaterials **32,** 8771, 2011.
36. Guimond, S.E., and Turnbull, J.E. Fibroblast growth factor receptor signalling is dictated by specific heparan sulphate saccharides. Curr Biol **9,** 1343, 1999.
37. Cool, S.M., and Nurcombe, V. The osteoblast-heparan sulfate axis: control of the bone cell lineage. Int J Biochem Cell Biol **37,** 1739, 2005.
38. Ornitz, D.M. FGFs, heparan sulfate and FGFRs: complex interactions essential for development. Bioessays **22,** 108, 2000.
39. Roberts, J.J., Nicodemus, G.D., Greenwald, E.C., and Bryant, S.J. Degradation improves tissue formation in (un)loaded chondrocyte-laden hydrogels. Clin Orthop Relat Res **469,** 2725, 2011.
40. Rice, M.A., and Anseth, K.S. Encapsulating chondrocytes in copolymer gels: bimodal degradation kinetics influence cell phenotype and extracellular matrix development. J Biomed Mater Res Part A **70,** 560, 2004.

Address correspondence to:
Fan Yang, PhD
Departments of Orthopaedic Surgery and Bioengineering
Stanford University School of Medicine
300 Pasteur Dr., Edwards R105
Stanford, CA, 94305-5341

E-mail: fanyang@stanford.edu

Received: July 26, 2016
Accepted: September 22, 2016
Online Publication Date: October 19, 2016